Dispersion relation for waves in the Belousov–Zhabotinsky reaction

Jean-Marc Flesselles,[a] Andrew Belmonte[b] and Vilmos Gáspár*[c]

[a] *Laboratoire PMMH-URR 7636 CNRS, École Supérieure de Physique et Chimie Industrielles de Paris, 10 rue Vauquelin, F-75231 Paris Cedex 05, France*
[b] *Department of Physics and Astronomy, University of Pittsburgh, Pittsburgh, PA 15260, USA*
[c] *Institute of Physical Chemistry, Kossuth L. University, H-4010 Debrecen, P.O. Box 7, Hungary*

Analysis of a chemical model for the Belousov–Zhabotinsky reaction leads to an analytic form for the dispersion relation for waves travelling in such a medium. It is found that the velocity varies as the hyperbolic tangent of the normalized period. Data analysis suggests that the normalization time is the selected spiral period for the medium. This result agrees with previously published data, one-dimensional as well as two-dimensional, all of which can be rescaled onto a single dimensionless curve. It thus provides a unifying approach to all waves in this reaction.

1 Introduction

Spiral waves are ubiquitous in spatially distributed chemical and biological systems whose local kinetics are excitable.[1] Such media include reaction–diffusion systems,[2] cardiac muscle tissue,[3,4] nerve axons[5] and aggregating slime mould cells.[6,7] Much experimental and theoretical work has been devoted to understanding the formation and dynamical properties of spiral waves in excitable media.[8–10] In particular, waves in heart tissue have been studied extensively since they are believed to play an essential role in heart diseases.[11] On the other hand, chemical systems, such as the well known Belousov–Zhabotinsky (BZ) reaction[12] or the surface-catalyzed oxidation of CO on platinum[13] have provided the most suitable media for controlled laboratory experiments.

A rotating spiral wave is a simple dynamical pattern characterized by two parameters:[14] pitch p and rotation period T. In excitable media such as the BZ reagent, periodic waves are known to travel at a speed $c(T)$ which depends upon the period of excitation. This relationship, known as the dispersion relation, is important to understanding the dynamics of one-or two-dimensional wave propagation. It also plays an essential role in the selection mechanism by which spirals in a given medium always develop a unique pitch p_s and period T_s.

Although there have been several measurements of the dispersion relation in various BZ media,[15–24] only recently was a successful rescaling discovered.[24] Specifically, it was found, in experiments on spiral waves, that an appropriate rescaling collapses all experimental data onto a single line M *vs. x*, resulting in a universal dimensionless plot for all spiral waves; $M = p^2/TD$ is the effective diffusion enhancement due to spiral wave propagation, where p^2/T is the so called internal diffusion coefficient of the spiral pattern, D is the characteristic diffusion coefficient of the BZ reagent, and $x = T/T_s$ is the rotation period normalized by the selected spiral period T_s. A linear fit of the dimensionless plot leads to an analytical form for the dispersion relation that provides a satisfactory fit,[24] but with neither theoretical nor chemical justification.

In this paper, we first derive an analytical form for the dispersion relation in the BZ reagent. The new formula is based on the analysis of a two-variable dynamical model for the BZ system and on general considerations for excitable reaction–diffusion media. We then briefly describe the details of our previous experiments, and reanalyse the results, together with other published dispersion curves for the BZ system, in terms of our formula. We show that the analytical form satisfactorily fits all previous data, and that an appropriate rescaling does indeed permit analysis and comparison in terms of the dimensionless variables x and M. Finally, we discuss the implications for further work on chemical waves.

2 Derivation of the dispersion relation

Currently, it is widely accepted that the spatio-temporal behaviour of two-dimensional BZ media can be described by the following set of coupled reaction–diffusion equations:

$$\varepsilon \frac{\partial u}{\partial t} = u(1-u) - fv\frac{u-q}{u+q} + \varepsilon^2 \nabla^2 u \tag{1}$$

$$\frac{\partial v}{\partial t} = (u-v) + \varepsilon\delta\nabla^2 v \tag{2}$$

eqn. (1) and (2) are based on the Tyson–Fife reduction[25] of the Oregonator model[26] for the BZ reaction. In the ferroin-catalysed BZ system, the variables u and v represent the dimensionless concentrations, respectively, of $HBrO_2$ (propagator species) and of the oxidized form of the catalyst–ferriin (controller species); t is dimensionless time, while $\varepsilon \ll 1$ is a constant relating the timescales of the fast u variable and the slow v variable; $\delta = D_v/D_u$ is the ratio of the corresponding diffusion coefficients and ∇^2 is the two-dimensional Laplacian in rescaled spatial coordinates. Values of the model-related parameters f and q depend upon the chemical constitution of the BZ reagent.[25]

However, recent experiments have shown that the Oregonator fails to describe spiral waves quantitatively.[14] In particular, the experimentally observed concentration effects of the main reactants (such as sodium bromate, sulfuric and malonic acids) are different than those predicted by the model. It, nevertheless, provides a satisfactory qualitative description of both the pattern itself, and to some extent of the chemistry involved. More specifically the excitable nature of the medium is properly reproduced, as well as the structure of the chemical front.

The excitable behaviour of eqn. (1) and (2) is related to the saw-tooth form of the u nullcline shown in Fig. 1(a). The system is at rest at the intersection of the two nullclines, where $u = u_r$ and $v = v_r$. Small perturbations rapidly relax to rest, but perturbations above a certain threshold move the system over the middle section of the u nullcline, and generate a propagating pulse. In the front of the pulse, the medium jumps
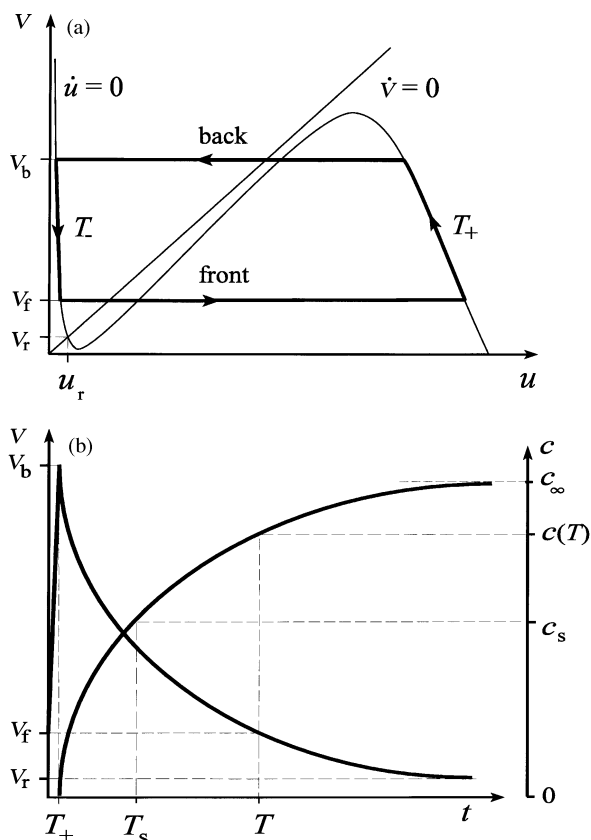
Fig. 1 (a) Sketch of the phase plane for model eqn. (1) and (2). Variables u and v define the instantaneous state of the system. Thin lines are the so-called nullclines. The u nullcline corresponds to the solution of $\dot{u} = 0$, where $\dot{u}$ stands for the right-hand side of eqn. (1) without the diffusion term. The v nullcline is calculated by using eqn. (2) without the diffusion term. The system is at rest at the intersection of the two nullclines (u_r, v_r). The thick line shows a typical phase-plane trajectory when periodic waves are generated in the medium. v_f and v_b indicate the constant levels of the controller variable v in the successive wavefronts and wavebacks, respectively. (b) Typical concentration profile of the slow v variable (left vertical axis) when a pulse sweeps through the medium. v_r is the value at rest, while v_b is the maximum value at T_+. When wave trains are generated with period T, the value of v drops from v_b to v_f only, then it jumps up again to v_b (not shown in the figure). The figure also shows the increase in the wave velocity c (right vertical axis) as an arbitrary function of the period of excitation. c_∞ is the maximum velocity in a given medium.

from the rest to an excited state (up), while in the back it relaxes to rest (down). Consequently, there are two waves: a wavefront and a waveback associated with the up- and down-jumps in the medium.

Tyson and Keener[8] have shown that the direction of a wave and its speed c are determined by the level of controller species v in front of the wave. Typically, $c(v)$ is a decreasing function of v: a high level of the controller species slows down the wave. It is important to note that $c(v)$ changes sign at some $v_* \in [v_r, v_{max}]$. When periodic perturbations are applied, the controller levels v_f and v_b in the successive wavefronts and wavebacks, respectively, approach constant values, such that the wavefronts and wavebacks travel at the same speed $c(v_f) = |c(v_b)|$. Thus the pattern becomes strictly periodic. The period T of the wave train is the sum of the durations of the up- and down-jumps, T_+ and T_-, respectively.

Fig. 1(b) shows a typical concentration profile of slow variable v when a pulse sweeps through the medium. As $T_+ \ll T_-$, an approximate value for period T can be calculated by solving:

$$T \approx T_- = \int_{v_b}^{v_f} \frac{dv}{(dv/dt)_-} \tag{3}$$

where $(dv/dt)_-$ is the rate equation for variable v during the down-jump. Since during the down-jump $u \ll v$, the rate equation from eqn. (2) is (neglecting the spatial variations):

$$(dv/dt)_- \approx -v/\tau \tag{4}$$

where τ is a relaxation time characterizing the kinetics in the back of the wave.† Substituting the right-hand side of eqn. (4) into eqn. (3), and evaluating the integral, leads to the following formula:

$$T \approx -\tau \ln \frac{v_f}{v_b} \tag{5}$$

We now make an additional assumption that both v_b and v_f remain close to v_*, *i.e.* the fronts travel slowly, and linearize

$$c(v) \approx -\alpha(v - v_*) \tag{6}$$

Since we impose that $c(v_b) = -c(v_f)$ with $v_f < v_* < v_b$, we can write $v_b = v_* + \Delta$, $v_f = v_* - \Delta$. Using these expressions for v_b and v_f in eqn. (5) yields:

$$\Delta = v_* \tanh(T/2\tau) \tag{7}$$

As the linearized wavefront velocity is $c = \alpha\Delta$, we finally get:

$$c(T) = c_\infty \tanh(T/T_*) \tag{8}$$

This equation is characterized by two parameters: c_∞, the velocity for infinitely spaced fronts, and T_*, a chemical time-scale. In principle, these parameters should be deduced from the model. Owing to our preceding remarks regarding the reliability of the Oregonator model, we will keep the functional form and consider these quantities as adjustable parameters.

The functional form of eqn. (8) has the expected global shape for the dispersion relation in BZ media:[27,28] the velocity increases slower than linearly for low periods and saturates for large T values. In addition, it naturally implies a scaling form for M. If we denote $\xi = T/T_*$, then

$$M = \beta\xi \tanh^2 \xi; \quad \text{with } \beta = c_\infty^2 T_*/D \tag{9}$$

3 Review of experiments and data analysis

The experimental determination of the dispersion relation for spiral waves in various BZ media[14,24] was performed using an open spiral reactor.[24,29] It is made of two continuously fed, well stirred tank reactors separated by a thin porous glass disk. Though chemical gradients exist perpendicular to the disk, pattern formation takes place only inside the disk, which is treated as a two-dimensional reaction–diffusion system. The advantage of using an open spatial reactor is that the composition of the medium does not change with time; thus true stationary patterns can be observed. On the other hand, the sensitivity of the ferroin-catalysed BZ system to visible light[30] allows us to impose a different period and pitch on the spiral without changing the chemical composition.

Local application of red laser light to the spiral core slows down the reaction in that region because of the light-induced production of bromide ions,[31] an inhibitor species of the BZ reagent. As the reaction becomes slower in the spiral core, the entire spiral rotates more slowly as the pitch increases. Fig. 2 shows the transient spiral shape after the laser beam has been turned on. Eventually the spiral reaches a new steady state. As the intensity of the laser beam is increased, the inhibitory effect also increases, resulting in even slower rotation and larger pitch. When the laser beam is turned off, the medium

---

† Note that, from this point onward, all variables and parameters are dimensional. However, for simplicity we do not introduce new symbols.

Fig. 2 Evolution of a spiral after the laser beam, focused at the spiral core, has been turned on. The spiral has a diameter of 20.25 mm. Concentrations are: $[H_2SO_4]_0 = 0.3$ M, $[NaBrO_3]_0 = 0.40$ M, $[MA]_0^A = 0.40$ M, $[NaBr]_0^A = 30$ mM, $[SDS]_0^A = 0.03$ mM and $[ferroin]_0^B = 1.0$ mM. Superscripts A and B designate the reactors into which the chemicals are introduced. MA: malonic acid, SDS: sodium dodecyl sulfate and ferroin: tris(1,10-*o*-phenanthroline)iron(II) complex ion.

recovers and the spiral returns to its selected pitch and period.[24]

The dispersion relation is constructed by plotting the wave speed $c(T)$ as a function of rotation period T. These spiral wavefronts provide an approximation to the dispersion relation for flat periodic waves in one- or two-dimensional BZ media. The velocity of a curved wavefront can be written as[27]

$$c_{2D}(T) = c(T) - D\kappa \qquad (10)$$

where $c(T)$ is the velocity of a plane wave, D is the diffusion constant of the medium, and κ is the curvature of the wavefront. In this experiment[14] $D \approx 4 \times 10^{-6}$ cm^2 s^{-1} and for a typical spiral $\kappa \approx 10$ cm^{-1} after one turn, which means that, over most of the spiral, the observed velocity p/T (≈ 10 μm s^{-1}) is approximately equal to the plane wave velocity $c(T)$. Measurements are made at least five turns from the spiral centre, where the curvature effects are negligible, so that the measured dispersion relation is that relevant to plane waves. Thus these experiments utilize the spiral only as a wave source. As long as there is no meandering, the results do not depend on the dynamics of the tip. This question has been treated elsewhere both theoretically[8,27] and experimentally.[14]

In Fig. 3(a), we represent the same experimental data as those of Fig. 4 in ref. 24. These data, numbered I–V, correspond to five different experimental conditions listed in Table 1. As the direct least-mean-square fits by eqn. (8) provide
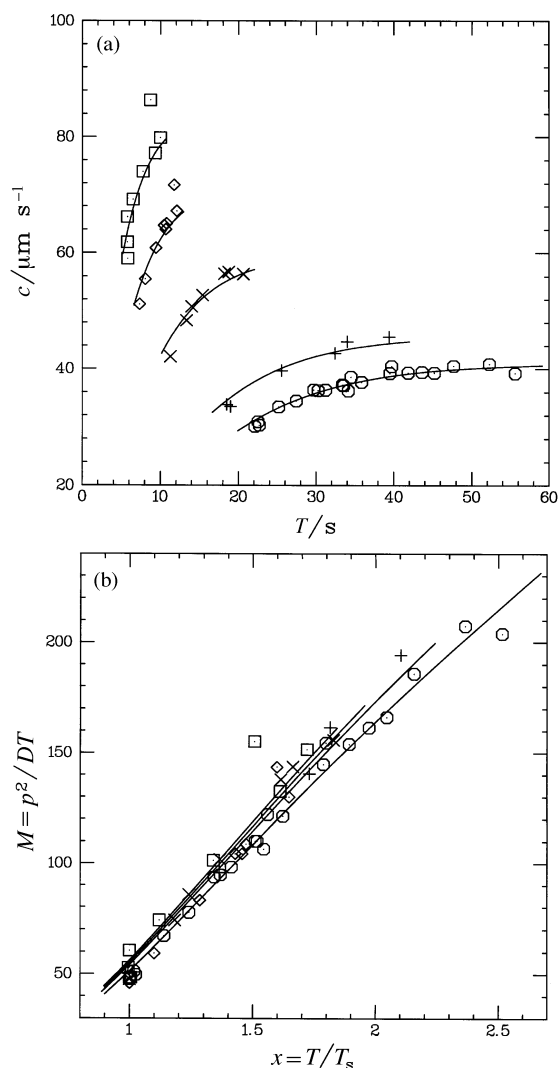

Fig. 3 (a) Speed $c(T)$ of spiral fronts as a function of rotation period T for data I–V. Solid lines are fits by eqn. (8). The fitted values are reported in Table 2. Symbols: ($+$) I, ($\times$) II, ($\diamond$) III, ($\square$) IV, ($\bigcirc$) V. (b) Same data as in (a) but represented as M vs. x.

values of T_* close to the selected spiral periods found in the experiments, it suggests the equality

$$T_* = T_s \qquad (11)$$

Thus, one could use x instead of ξ. This constraint has been imposed to fit c_∞. The fitting values are summarized in Table 2. As seen in Fig. 3(a), eqn. (8) with constraint (11) gives an

Table 1 Characteristics of the analysed experimental data

#	ref.	$[H_2SO_4]$/M	$[BrO_3^-]$/M	$[MA]$/M	$[ferroin]$/mM	conditions	pattern
I	24	0.2	0.4	0.4	1.0	open CSTR	2D spiral
II	24	0.3	0.4	0.4	1.0	open CSTR	2D spiral
III	24	0.4	0.4	0.4	1.0	open CSTR	2D spiral
IV	24	0.5	0.4	0.4	1.0	open CSTR	2D spiral
V	24	0.4	0.15	0.2	1.0	open CSTR	2D spiral
A	19	0.18	0.33	0.12	2.9	closed capillary	1D
B	20	0.2	0.31	0.08	2	closed Petri	2D target
C	21	0.21?	0.22	0.048?	3.8	Petri	2D target
D	17	0.34	0.31	0.12	2.9	agar gel	2D spiral
E	18	0.77	0.57	0.33	$Ru(bpy)_3^{2+}$	silica gel	2D spiral
F	22	0.2	0.25	0.05	in resin	in resin	2D spiral
G	15	0.38	0.39	0.095	3.5	closed Petri	2D target
H	23	<0.2	<0.3	<0.025	2.25	PA gel	quasi 1D

Table 2 Measured and fitted values used in figures

	experimental values			fitted values				
#	T_s/s	c_s/µm s^{-1}	c_∞/µm s^{-1}	T_s^F/s	c_s^F/µm s^{-1}	c_∞^F/µm s^{-1}	D/µm^2 s^{-1}	$M(1)$
I	18.7	33.7		*18.7*	34.8	**45.7**	420	54
II	11.3	42.1		*11.3*	45.3	**59.5**	420	55
III	7.3	51.0		*7.3*	54.1	**71.1**	420	51
IV	5.8	64.0		*5.8*	63.7	**83.7**	420	56
V	22.1	30.4		*22.1*	31.2	**41.0**	420	51
A	60–75	46.7	79.2	**79.0**	60.3	79.2	2000	144
B	>28		90.3	**39.6**	68.8	90.3	2000	96
C	>81.4	>45.3	56.7	**94.9**	43.2	56.7	2000	88
D	19–22	55	125	**21.6**	95.2	*125*	1500	131
E	26	49.6		*26*	62.3	**81.7**	1500	67
F			35	**146**	26.7	*35*	1000	104
G	17.3	76	125	**21.9**	87.5	**114.9**	1900	88
H	>1225	>6.33	<15.7	**3576**	13.0	**17.1**	1000	607

Quantities written in italics have been imposed, while those in bold have been fitted; c_s^F and $M(1)$ values have been deduced from the fits. Numbers I to V and letters A to H refer to conditions given in Table 1.

excellent fit (solid curves) to the data. However, the analysis of data in Table 2 shows that the resulting value for c_s is systematically a few per cent higher than the measured one. This point will be addressed later.

We also represent the same data in Fig. 3(b), using the $M(x)$ representation. The continuous lines correspond to the same curves that directly fit $c(T)$ in Fig. 3(a). The slight variations arise from the small dispersion of $M(1)$. Note that the actual value of the diffusion coefficient is necessary to compute M. We have used $D = 4.2 \times 10^{-6}$ cm^2 s^{-1}.[14] This value, smaller than the earlier reported value for BZ systems in solution, has been measured for the BZ media in the porous glass disk of the open reactor used in ref. 24.

Assuming that $T_* = T_s$ has important consequences; in particular, it fixes the ratio c_s/c_∞ at tanh (1) $\approx$ 0.76. This value is larger than the previously estimated ratio of 0.62 that arose from a linear fit of M.[24] However, as can be checked using Fig. 3(b), both ratios are compatible with the data owing to the small variation of the hyperbolic tangent for arguments greater than 1.

4 Comparison with other data

In order to check eqn. (8) and (9) with the constraint (11), we compare a number of published experimental dispersion relations obtained in various experimental conditions in the BZ reaction. Ševčíková and Marek[16] provided the first attempt to compare experimental results quantitatively with theoretical predictions[28] which, at that time, arose from the Oregonator. They concluded that a proper agreement was still lacking. We consider those analysed in ref. 16 and add four more articles.[15,18,22,23] The different characteristics and experimental conditions of the data we compare are summarized in Table 1.

All experiments but one (H) were run in batch reactors, where the system ages; this was pointed out in ref. 17. All concentrations are different; sometimes bromide was also added. Ferroin was used as the catalyst in all cases except E, where ruthenium bipyridyl was used instead. Some curves have been measured in thin layers of BZ solutions (B, C and G), one in a capillary (A), whereas others have been obtained in different kinds of immobile media, either silica gel (E), agar gel (D), polyacrylamide gel (H) or resin (F). Experiment H is markedly peculiar, since permanent gradients are established within the reaction domain; its timescales are an order of magnitude longer than the others. Finally, satisfactory data for the corresponding spiral in the same experimental conditions are available in a few cases only: A (but the spiral has not been done in a capillary), D (but the spiral was meandering, hence its period and front velocities were ill defined), E

(but the dispersion curve was only roughly obtained), and G (but a different batch had apparently been used). However, all dispersion curves have the same characteristic shape described earlier.

The actual values of c and T have been obtained by copying the published dispersion curves and measuring them off the graphs. In order to fit the data, we have imposed the known quantities to be those found experimentally. For data sets A to D and F we have imposed the measured values of c_∞. For experiment E the known value of T_s has been imposed instead. In the case of G both T_s and c_∞ were known, but direct substitution into eqn. (8) did not give a satisfactory fit. Hence, for this one and for H, where not values but rather bounds on them were given, we fitted both T_s and c_∞. The results are reported in Table 2 and represented in Fig. 4. As can be seen, most data are well fitted. Two sets only seem to depart slightly: D and F. In the former case, this may be due to the meandering of the spiral. In the latter case, it just falls within the large dispersion of the experimental data (see Fig. 2 in ref. 22). Note that the fit for H does not appear in Fig. 4 because the timescales are significantly larger, however, the obtained fit is of similar quality.

A direct check of eqn. (9) requires more care. Once T_s is set, the scaling variable x is given. Then the value of M only depends on β, which is a function of T_s and c_∞, both being
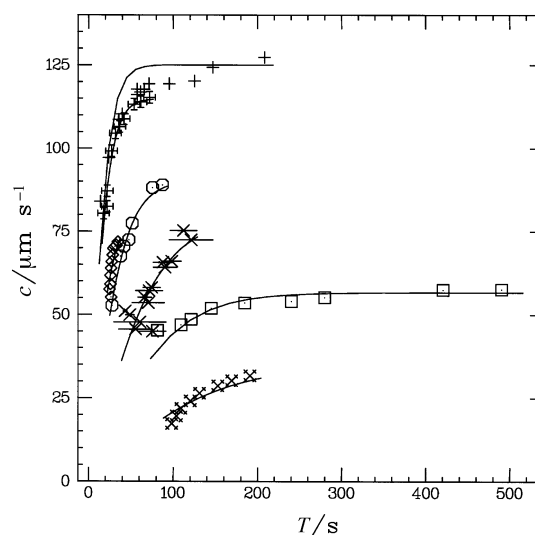

Fig. 4 Speed $c(T)$ of periodic waves as a function of excitation period T for data A–G. Solid lines are fits by eqn. (8). The fitted values are reported in Table 2. Symbols: ($\times$) A, ($\bigcirc$) B, ($\square$) C, ($+$) D, ($\diamond$) E, ($\otimes$) F, ($\ast$) G.
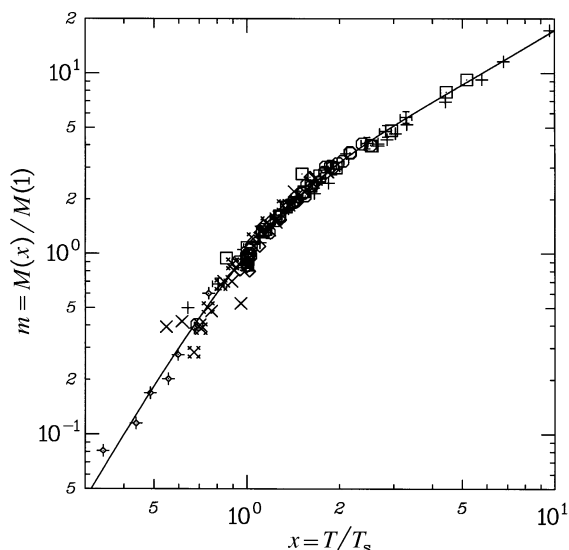
Fig. 5 Dimensionless plot of $m = M(x)/M(1)$ *vs.* x for all data in Table 1. The solid curve corresponds to the theoretical fit imposed by eqn. (8). Symbols are as in Fig. 3 and 4, and ($\diamondsuit$) H.

fixed by the fit of the dispersion curve, and also of the diffusion coefficient D. This coefficient, which sets the absolute scale of M, cannot be deduced from the dispersion relation data. In Table 2, we report the diffusion coefficients we have used (and guessed somewhat arbitrarily when not available) and the values of $M(1)$ that have been calculated from the fits. There is a rather large dispersion for the values of $M(1)$, in seeming contradiction with claims of a limited available range.[14,24,32,33] However, the controversy on this matter is not yet settled. In addition, the true values for the diffusion coefficients are hardly available and could easily be overestimated by a factor of 3. This would bring all $M(1)$ closer. The case of H should be considered separately, because of its particular geometry; although the dispersion relation should apply, since it is characteristic of the medium, there is no reason to find a spiral value for $M(1)$.

Hence, to check the functional form of eqn. (9), we have normalized $M(x)$ by $M(1)$ to eliminate the diffusion coefficient. Plotted in log–log in Fig. 5 is $m(x) = M(x)/M(1)$ for all analysed data (13 experimental dispersion curves). For this plot, the only fitted quantity is T_s used to normalize the periods in x. The solid curve corresponds to the theoretical fit imposed by eqn. (8). The agreement is excellent.

5 Conclusion

Starting from model equations for the BZ reaction, we have derived a dispersion relation which states that the velocity varies as the hyperbolic tangent of the normalized period. Data analysis suggests that the normalization time is the selected spiral period for the medium. This explains the scaling observed experimentally in ref. 24. Though the functional form of the dispersion relation has been obtained by considerable simplifications, it, nevertheless, provides an excellent fit to a large number of available published data.

However, a more detailed analysis of the data shows that the experimentally observed velocities at selection are slightly different from the predicted ones, increasingly so as the selected period becomes smaller. This may mark the validity limits of our analysis. Indeed, for small periods, it is likely that T_+ is no longer negligible with respect to T_-. Although a refined theory is still required in this limit, we might say that we are now beginning to have a unifying approach to dispersion curves for the BZ reaction.

References

1   *Waves and Patterns in Chemical and Biological Media*, ed. H. Swinney and V. Krinsky, *Physica D*, 1991, **49**.
2   *Chemical Waves and Patterns*, ed. R. Kapral and K. Showalter, Kluwer, Dordrecht, 1995.
3   A. T. Winfree, *When Time Breaks Down*, Princeton University Press, 1987.
4   J. Davidenko, A. Pertsov, R. Salomonsz, W. Baxter and J. Jalife, *Nature (London)*, 1992, **355**, 349.
5   A. L. Hodgkin and A. F. Huxley, *J. Physiol.*, 1952, **117**, 500.
6   G. Gerisch, *Naturwissenschaften*, 1983, **58**, 420.
7   K. J. Lee, E. C. Cox and R. E. Goldstein, *Phys. Rev. Lett.*, 1996, **76**, 1174.
8   J. J. Tyson and J. P. Keener, *Physica D*, 1988, **32**, 327.
9   V. A. Davidov, V. S. Zykov and S. Mikhailov, *Sov. Phys. Usp.*, 1991, **34**, 665.
10 E. Meron, *Phys. Rep.*, 1992, **218**, 1.
11 A. Winfree, *Science*, 1995, **270**, 1224.
12 A. Zaikin and A. Zhabotinsky, *Nature (London)*, 1970, **225**, 535.
13 S. Jakubith, H. Rotermund, W. Engel, A. von Oertzen and G. Ertl, *Phys. Rev. Lett.*, 1990, **65**, 3013.
14 A. Belmonte, Q. Ouyang and J-M. Flesselles, *J. Phys. II*, 1997, **7**, 1425; *J. Physique (Paris)*, 1997, **7**, 1917.
15 P. Foerster, S. C. Müller and B. Hess, *Proc. Natl. Acad. Sci. USA*, 1989, **86**, 6831.
16 H. Ševčíková and M. Marek, *Physica D*, 1989, **39**, 15.
17 W. Jahnke, W. E. Skaggs and A. T. Winfree, *J. Phys. Chem.*, 1989, **93**, 740.
18 O. Steinbock and S. C. Müller, *Physica A*, 1992, **188**, 61.
19 A. T. Winfree, unpublished data, 1973, reproduced in ref. 27, 28.
20 A. Pagola, J. Ross and C. Vidal, *J. Phys. Chem.*, 1988, **92**, 163.
21 M. Marek and H. Ševčíková, in *From Chemical to Biological Organization*, ed. M. Markus, S. C. Müller and G. Nicolis, Springer, Berlin, 1988, p. 103.
22 C. Oosawa, Y. Fukuta, K. Natsune and K. Kometani, *J. Phys. Chem.*, 1996, **100**, 1043.
23 E. Dulos, J. Boissonade and P. De Kepper, in *Nonlinear Wave Processes in Excitable Media*, ed. A. V. Holden, M. Markus and H. G. Ohmer, Plenum Press, New York, 1991, p. 423.
24 A. Belmonte and J-M. Flesselles, *Phys. Rev. Lett.*, 1996, **77**, 1174.
25 J. J. Tyson and P. C. Fife, *J. Chem. Phys.*, 1980, **73**, 2224.
26 R. J. Field and R. M. Noyes, *J. Chem. Phys.*, 1974, **60**, 1877.
27 J. P. Keener and J. J. Tyson, *Physica D*, 1986, **21**, 307.
28 J. D. Dockery, J. P. Keener and J. J. Tyson, *Physica D*, 1988, **30**, 177.
29 Q. Ouyang and H. Swinney, *Chaos*, 1991, **1**, 411.
30 V. Gáspár, G. Bazsa and M. Beck, *Z. Phys. Chem. (Leipzig)*, 1983, **264**, 43.
31 H. J. Krug, L. Pohlmann and L. Kuhnert, *J. Phys. Chem.*, 1990, **94**, 4862.
32 A. Karma, *Phys. Rev. Lett.*, 1992, **68**, 397.
33 A. T. Winfree, *Physica D*, 1991, **49**, 125.